

# *Chlamydia trachomatis* recombinant MOMP encapsulated in PLGA nanoparticles triggers primarily T helper 1 cellular and antibody immune responses in mice: a desirable candidate nanovaccine

Stacie J Fairley  
Shree R Singh  
Abebayehu N Yilma  
Alain B Waffo  
Praseetha Subbarayan  
Saurabh Dixit  
Murtada A Taha  
Chino D Cambridge  
Vida A Dennis

Center for NanoBiotechnology  
Research, Alabama State University,  
Montgomery, AL, USA

**Abstract:** We recently demonstrated by in vitro experiments that PLGA (poly D, L-lactide-co-glycolide) potentiates T helper 1 (Th1) immune responses induced by a peptide derived from the recombinant major outer membrane protein (rMOMP) of *Chlamydia trachomatis*, and may be a promising vaccine delivery system. Herein we evaluated the immune-potentiating potential of PLGA by encapsulating the full-length rMOMP (PLGA-rMOMP), characterizing it in vitro, and investigating its immunogenicity in vivo. Our hypothesis was that PLGA-rMOMP triggers Th1 immune responses in mice, which are desirable prerequisites for a *C. trachomatis* candidate nanovaccine. Physical-structural characterizations of PLGA-rMOMP revealed its size (approximately 272 nm), zeta potential (−14.30 mV), apparent spherical smooth morphology, and continuous slow release pattern. PLGA potentiated the ability of encapsulated rMOMP to trigger production of cytokines and chemokines by mouse J774 macrophages. Flow cytometric analyses revealed that spleen cells from BALB/c mice immunized with PLGA-rMOMP had elevated numbers of CD4+ and CD8+ T cell subsets, and secreted more rMOMP-specific interferon-gamma (Th1) and interleukin (IL)-12p40 (Th1/Th17) than IL-4 and IL-10 (Th2) cytokines. PLGA-rMOMP-immunized mice produced higher serum immunoglobulin (Ig)G and IgG2a (Th1) than IgG1 (Th2) rMOMP-specific antibodies. Notably, sera from PLGA-rMOMP-immunized mice had a 64-fold higher Th1 than Th2 antibody titer, whereas mice immunized with rMOMP in Freund's adjuvant had only a four-fold higher Th1 than Th2 antibody titer, suggesting primarily induction of a Th1 antibody response in PLGA-rMOMP-immunized mice. Our data underscore PLGA as an effective delivery system for a *C. trachomatis* vaccine. The capacity of PLGA-rMOMP to trigger primarily Th1 immune responses in mice promotes it as a highly desirable candidate nanovaccine against *C. trachomatis*.

**Keywords:** *Chlamydia trachomatis*, bacteria, vaccine, antibody, cytokines, PLGA nanoparticles

## Introduction

*Chlamydia trachomatis* is the most common sexually transmitted bacterium in both developed and developing countries, which makes it of serious public health concern.<sup>1,2</sup> Reports from the Centers for Disease Control and Prevention state that more than 90 million new cases occur each year.<sup>1-4</sup> Over 75% of women and 50% of men are asymptomatic<sup>5,6</sup> and therefore do not seek medical treatment.<sup>1,3,7,8</sup> Currently, the most common control method for *C. trachomatis* infection is the use of antibiotics.

Correspondence: Vida A Dennis  
Center for NanoBiotechnology  
Research, Alabama State University,  
1627 Hall Street, Montgomery,  
AL 36104, USA  
Tel +1 334 229 8447  
Email vdennis@alasu.edu

However, the asymptomatic nature of the bacterium precludes early detection, thus making use of antibiotics problematic. Moreover, antibiotics do not always protect against established infections or reinfection. If left untreated, *C. trachomatis* infection can result in pelvic inflammatory disease, ectopic pregnancy, infertility, and epididymitis.<sup>9,10</sup> The global cost associated with treating infected patients has reached in excess of 10 billion dollars annually.<sup>11–13</sup>

Because antibiotic treatment of *C. trachomatis* is effective only during early infection, and does not prevent reinfection, there is a general consensus in the field that the best approach to controlling this bacterial infection is a vaccine. However, the challenge in development of *C. trachomatis* vaccine is selection of an immunogen, its delivery, and the capacity of the immunogen to mount an immune response, which will provide long-term protective resistance against infection. In the early 1950s, vaccines were developed using live, inactivated, or attenuated whole *C. trachomatis*.<sup>14–20</sup> Although these vaccines offered some degree of protection, the costs associated with production, the complexity of protection, and the possibility of the bacteria reverting to virulent forms made them far from ideal as candidate nanovaccines. To avoid the harmful effects associated with these earlier forms of vaccines, subunit proteins have become attractive alternatives as a candidate vaccine against *C. trachomatis*.

To date, the most promising subunit candidate vaccine is the major outer membrane protein (MOMP) of *C. trachomatis*.<sup>21–25</sup> MOMP accounts for 60% of the outer membrane mass of *C. trachomatis* and is considered an ideal candidate because it contains many antigenic T cell and B cell epitopes.<sup>26,27</sup> Nonetheless, vaccine research with MOMP as the prime immunogen has been both encouraging and disappointing. Previous studies using native MOMP in combination with adjuvant revealed some protective efficacy in vivo,<sup>28–30</sup> but the drawback with native MOMP is the expense associated with its production if selected as a candidate vaccine.<sup>16</sup> The use of recombinant MOMP (rMOMP) with conventional adjuvants, including cholera toxin, aluminum, and CpG, to name a few, has been widely explored, but the degree of protection achieved with these vaccines is not as robust as that achieved with native MOMP.<sup>31–35</sup>

A promising alternative to using adjuvant is encapsulation of an immunogen in biodegradable polymers approved by the US Food and Drug Administration that release their contents over time.<sup>36–45</sup> Among the approved biodegradable polymers, poly D, L-lactide-co-glycolide (PLGA) nanoparticles have advantages that include enhancement of immune responses,<sup>9–42</sup> delivery, biocompatibility and biodegradability,

size, and sustained release.<sup>38,43,44</sup> Several studies have shown the efficiency of this release system when used to encapsulate other peptides, proteins, or DNA.<sup>39–44</sup> Additionally, a study by Champion et al showed the protective efficacy of MOMP in a vault nanoparticle.<sup>46</sup> The uniqueness of PLGA versus other biodegradable nanoparticles is that it undergoes nonenzymatic hydrolysis, resulting in two biological metabolic byproducts, namely lactic acid and glycolic acid. We recently reported that a peptide derivative of rMOMP encapsulated in PLGA 85:15 had a slow release profile which triggered T helper (Th)1 responses in vitro using mouse J774 macrophages.<sup>44</sup> Moreover, we showed that these responses were potentiated by the presence of PLGA as the delivery system. In the present study, we encapsulated full-length rMOMP in PLGA 50:50 and subjected it to in vitro physical-structural characterization and immunogenicity studies using mouse J774 macrophages. Additionally, we assessed the immunogenicity of PLGA-rMOMP in BALB/c mice. We hypothesize that PLGA-rMOMP will trigger Th1 immune responses in mice, which are desirable prerequisites for a candidate *C. trachomatis* vaccine. Our data show the successful encapsulation of rMOMP in PLGA and that PLGA potentiates the production of cytokines and chemokines, as elicited by encapsulated rMOMP in macrophages. Of major significance, encapsulated rMOMP induced heightened cellular and antibody Th1 immune responses in mice. The potential of PLGA-rMOMP as a candidate nanovaccine against *C. trachomatis* is discussed herein.

## Materials and methods

### Cloning, expression, and purification of rMOMP

Polymerase chain reaction amplification of the full-length MOMP was performed following previously published methods<sup>35</sup> using Phusion Taq DNA polymerase (New England Biolabs, Ipswich, MA, USA) and the following primers: forward 5'-CGAACAGATTGGAGGTAAAAACTCTT-GAAATCGGTATTAG-3' and reverse 5'-CACGCGGCCGCT-TAGAAGCGGAATTGTGC-3' and ligated in pESUMO plasmid using T4 ligase kit (Life Technologies, Grand Isle, NY, USA). The plasmid was sequenced (Auburn University Genomics and Sequencing Laboratory, Auburn, AL, USA) and subsequently transformed into Rosetta (DE3) *Escherichia coli*-competent cells for protein expression. The apparent molecular weight and purity of rMOMP were determined by separation of protein extracts using 4%–20% ready linear gradient sodium dodecyl sulfate gels (BioRad Laboratories, Hercules, CA, USA), stained with Coomassie brilliant blue

(BioRad) and imaged using an Odyssey imaging system (Li-Cor, Lincoln, NE, USA). The protein was purified using a nickel affinity purification kit (Qiagen, Valencia, CA, USA) under denaturing conditions, as previously described.<sup>35</sup> The specificity of the purified rMOMP was confirmed by Western blotting<sup>35</sup> using anti-MOMP polyclonal antibodies (Fitzgerald Industries, Concord, MA, USA) followed by an Alexa Fluor 680 antibody (Life Technologies). Bound antibody was visualized using the Odyssey imaging system. The purified rMOMP preparation was also free of endotoxin activity, as assessed by polymyxin B experiments (data not shown).

## Fabrication of nanoparticles

PLGA 50:50 (molecular weight 30,000–60,000, Sigma-Aldrich, St Louis, MO, USA) nanoparticles were prepared using a modified w/o/w emulsion evaporation technique.<sup>44</sup> Briefly, PLGA (1%) and rMOMP (at a concentration of 500 µg in phosphate-buffered saline) were dissolved in dichloromethane (Sigma-Aldrich) and sonicated at a continuous mode for two minutes at 20-second intervals on ice, with the resulting emulsion added to an aqueous solution of 1% polyvinyl alcohol (molecular weight 85,000–124,000, Sigma) and sonicated again. The emulsion was stirred overnight at room temperature and the nanoparticles obtained by ultracentrifugation were washed three times with deionized water to remove excess polyvinyl alcohol, and then lyophilized (Lab Conoco, Kansas City, MO, USA) in the presence of 5% trehalose (as a stabilizer) to obtain PLGA-rMOMP. An equivalent volume of phosphate-buffered saline solution (as used for rMOMP) was similarly encapsulated in PLGA to serve as a negative control (PLGA-PBS). All lyophilized nanoparticles were stored at –80°C until used.

The encapsulation efficiency was extrapolated from measurements of the total protein encapsulated into PLGA as described previously.<sup>44</sup> Briefly, 20 mg of lyophilized PLGA-rMOMP was added to 1 mL of 0.1 N NaOH containing 2% sodium dodecyl sulfate and shaken overnight at room temperature. The supernatants were collected after centrifugation at  $13,680 \times g$  for five minutes and stored at –20°C. A micro bicinchoninic acid protein assay was used to quantify rMOMP in the supernatants, and absorbance was read at 570 nm using a microplate reader (Tecan US Inc, Durham, NC, USA). Background readings were corrected by subtracting the optical density values of supernatants from PLGA-PBS. The rMOMP encapsulation efficiency (EE) was calculated using the following formula:

$$EE = A-B/A \times 100$$

where A is the total amount of rMOMP and B is the free amount of rMOMP. These measurements were performed three times.

## In vitro studies

### Physical-structural characterization of nanoparticles

The encapsulated nanoparticles were characterized for their size, zeta potential, composition, and encapsulation efficiency following previously published methods.<sup>44,45</sup> Particle size and zeta potential measurements were obtained using a Malvern Zeta Sizer Nano ZS (Malvern Instruments Ltd, Worcestershire, UK). For each sample, a specific amount of nanoparticles was suspended in filtered water and sonicated prior to determinations of particle size and zeta potential. The results were expressed as the mean of triplicate runs.

### Surface morphology and ultraviolet visualization

Both scanning electron microscopy (SEM, Zeiss Evo, Thornwood, NY, USA) and transmission electron microscopy (TEM, Zeiss EM10) were used to ascertain surface morphology and size, following previously published methods.<sup>44</sup> TEM and SEM samples were prepared by placing one drop of diluted nanoparticle suspension on a carbon-coated grid or metal stub. The drop was allowed to dry at room temperature prior to microscopic analysis.

Ultraviolet visualization was used to ascertain the encapsulation of rMOMP in PLGA. For this study, nanoparticles were diluted in deionized water and their absorbance and spectral wavelength were used to determine whether absorption occurred on the outside of the nanoparticle.

### Release of encapsulated-rMOMP

In vitro release of rMOMP from the PLGA nanoparticles was determined as described.<sup>44</sup> In brief, encapsulated-rMOMP (250 µg/mL) was resuspended in phosphate-buffered saline containing 0.01% sodium azide and the tubes incubated at 37°C. At predetermined time intervals, the tubes were centrifuged, the supernatants were removed from the nanoparticles followed by replenishment of the same volume of fresh phosphate-buffered saline to nanoparticles. The protein quantity in collected aliquots was analyzed by bicinchoninic acid and read using a Tecan Sunrise microplate reader (Tecan Group Ltd, Morrisville, NC, USA). The protein released was also observed by Western blotting using the same procedure as described above.

### Stimulation of macrophages with nanoparticles

Mouse J774 macrophages were obtained from the American Type Culture Collection (Waldorf, MD, USA) and propagated

in Dulbecco's modified Eagle's culture medium at 37°C in a 5% CO<sub>2</sub> atmosphere.<sup>44</sup> Macrophages (1 × 10<sup>6</sup>/mL) were seeded in 12-well plates and stimulated with PLGA-rMOMP 10 µg/mL in the presence or absence of polymyxin B 10 µg/mL for 24 hours to determine the presence of any endotoxin activity. We elected to use PLGA-rMOMP at 10 µg/mL for this study because we previously observed that 10 µg/mL of purified rMOMP elicited production of cytokines by mouse J774 macrophages. Stimulation of macrophages with lipopolysaccharide 1 µg/mL served as a control for these experiments. The supernatants were collected by centrifugation after 24 hours and used to detect the interleukin (IL)-6 cytokine by specific cytokine enzyme-linked immunosorbent assay.<sup>44</sup>

Confocal analysis was used to confirm visually the bioactivity of PLGA-rMOMP in triggering secretion of IL-6 and IL-12p40 in macrophages. For these experiments, macrophages (1 × 10<sup>5</sup>/well) were seeded in eight-chamber well slides (BD Bioscience, Franklin Lakes, NJ, USA) and stimulated for 24 hours with PLGA-rMOMP 10 µg/mL or the equivalent weight of PLGA-PBS. The cells were washed with phosphate-buffered saline, fixed with paraformaldehyde for five minutes at 37°C, permeabilized using 0.1% Triton X and then blocked for two hours with 5% normal goat serum (Life Technologies). The cells were next stained with PE antimouse IL-6 (BD Bioscience) or FITC antimouse IL-12p40 diluted in normal goat serum for one hour, washed, and then counterstained with 4',6-diamidino-2-phenylindole (DAPI) combined with antifade mounting solution (Invitrogen, Carlsbad, CA, USA) according to the manufacturer's protocol. Cytokines were visualized using a Nikon Eclipse Ti confocal microscope (Nikon Instrument, Melville, NY, USA).

Because our previous study had revealed that as little as 1 µg/mL of a rMOMP peptide encapsulated in PLGA induced cytokine responses in macrophages,<sup>44</sup> we next determined the potentiating capacity of PLGA in the encapsulated rMOMP formulation by performing dose-response kinetics experiments using a concentration lower than 1 µg/mL of encapsulated rMOMP. Macrophages were either left unexposed or exposed to various concentrations of PLGA-PBS or PLGA-rMOMP (0.01, 0.1, 1, 10, and 100 ng/mL) or to rMOMP (0.5, 1, 10 and 20 µg/mL) for 24 hours, and the cell-free supernatants were collected and used to quantify IL-12p40.<sup>44</sup>

For some experiments, macrophages were stimulated with PLGA-PBS or PLGA-rMOMP and the cell-free supernatants were used for simultaneous quantification of several cytokines (IL-10, IL-1α, granulocyte-macrophage colony-stimulating factor, IL-15, granulocyte colony-stimulating factor, tumor

necrosis factor) and chemokines (CCL4, CCL2, CCL5, CXCL5, CXCL10) using a multiplex enzyme-linked immunosorbent assay (Millipore Corporation, Billerica, MA, USA). Data were acquired on a Luminex 100 system and analyzed using Bio-Plex Manager software version 4.1 (BioRad).

## In vivo studies

### Mice and immunization

Female 6–8-week-old BALB/c mice (Charles Rivers, Raleigh, NC, USA) were used for this study. The animal studies were performed following a protocol approved by the Alabama State University institutional animal care and use committee. The mice were housed under standard pathogen-free environmental conditions at ambient temperatures of 25°C, and provided with sterile food and water ad libitum. Groups of mice (n = 3 per group) received three immunizations at two-week intervals with phosphate-buffered saline, PLGA-PBS, or PLGA-rMOMP according to the methods described by Singh et al,<sup>35</sup> except via the subcutaneous route. Mice in the PLGA-rMOMP group were each immunized with 50 µg/200 µL of encapsulated rMOMP in phosphate-buffered saline, and those in the PLGA-PBS group were immunized with an equivalent weight of PLGA-PBS nanoparticles. The control mice were immunized with phosphate-buffered saline only. Two weeks following the last immunization, the mice were sacrificed to collect blood and spleen tissue for antibody and cytokine analyses, respectively.

### Flow cytometry

Single spleen cell suspensions were obtained from mice two weeks following the last immunization and pooled per group according to previous reports.<sup>47,48</sup> Spleen cells (1 × 10<sup>6</sup>/mL) were blocked with Fc blocking antibody (BD Bioscience) in fluorescent-activated cell sorting (FACS) buffer (phosphate-buffered saline, 0.1% NaN<sub>3</sub>, 1.0% fetal bovine serum) for 15 minutes at 4°C. The cells were washed and stained with fluorochrome-conjugated antibodies against lymphocyte surface receptors, FITC-CD8, and PE-CD4 (BD Biosciences) for 30 minutes at 4°C. The cells were then washed and fixed with 2% paraformaldehyde solution for 20 minutes at 4°C. Data were acquired on a BD FACS Canto II flow cytometer (BD Bioscience) with at least 1 × 10<sup>5</sup> events for each sample and analyzed using Flo Jo software (Tree Star Inc, Ashland, OR, USA).

### Quantification of cytokines

Spleen cell suspensions as collected above were pooled per group of mice and cultured as described.<sup>47,48</sup> Briefly, spleen

cells ( $3 \times 10^6$ /mL) were seeded into 12-well flat bottom tissue culture plates and stimulated with various concentrations of purified rMOMP (5 and 10  $\mu$ g/mL) and incubated at 37°C in a 5% CO<sub>2</sub> atmosphere. Cell-free supernatants were collected by centrifugation after 24 hours for quantification of Th1/Th17 (IL-12p40), Th1 (interferon gamma [IFN- $\gamma$ ]), and Th2 (IL-10 and IL-4) cytokines using specific cytokine enzyme-linked immunosorbent assays.

### Antibody determination

Sera collected two weeks following the last immunization from the groups of mice were pooled and used to detect anti-rMOMP-specific antibody responses as previously described,<sup>35,49</sup> except that 5  $\mu$ g/mL of purified rMOMP was used to coat plates in the present study. To determine antibody concentrations (titers), two-fold serial dilutions of serum were made and added to appropriate wells, followed by addition of either horseradish peroxidase-conjugated goat antimouse immunoglobulin (Ig) G, Ig2a, or IgG1 (Southern Biotech, Birmingham, AL, USA) antibody at a dilution of 1:2000. Plates were washed and developed using TMB substrate (KPL, Gaithersburg, MD, USA). Absorbance was read at 450 nm and the endpoint titer was considered to be the last serum dilution with readings higher than the mean + 3 standard deviations of negative control sera.

### Statistical analysis

Cytokine and antibody data were analyzed using the two-tailed unpaired Student's *t*-test.  $P < 0.05$  was considered to be statistically significant.

## Results

### Expression and purification of rMOMP

Expression of rMOMP in Rosetta (DE3) *E. coli* resulted in a protein of about 52 kDa extracted from the pellet as predicted from the molecular weight marker (Figure 1 A–C, lane 1). Pooled fractions were analyzed by sodium dodecyl sulfate polyacrylamide gel electrophoresis and stained with Coomassie Brilliant Blue (Figure 1A, lane 2). Purification of the pooled fractions resulted in a protein band of about 52 kDa (Figure 1B, lane 2), corresponding to the expected size of rMOMP. Proteins transferred to the nitrocellulose membrane and probed with anti-MOMP polyclonal antibodies confirmed the specificity of purified rMOMP of about 52 kDa (Figure 1C, lane 2).

### Physical-structural characterization of nanoparticles

Previously we developed a modified w/o/w double emulsion technique by adding trehalose prior to lyophilization for stabilization of nanoparticles.<sup>44</sup> A schematic of the encapsulation of rMOMP in PLGA is depicted in Figure 2A. Use of this method in the present study aided the stability of PLGA-rMOMP with a zeta potential of  $-14.3$  mV as compared with  $-24.8$  mV for PLGA-PBS, with an encapsulation efficiency of approximately 60%, and average sizes of 224 nm (PLGA-PBS) and 272 nm (PLGA-rMOMP, Table 1).

Both TEM and SEM analyses of PLGA-PBS (Figure 2B and D) and PLGA-rMOMP (Figure 2C and E) revealed

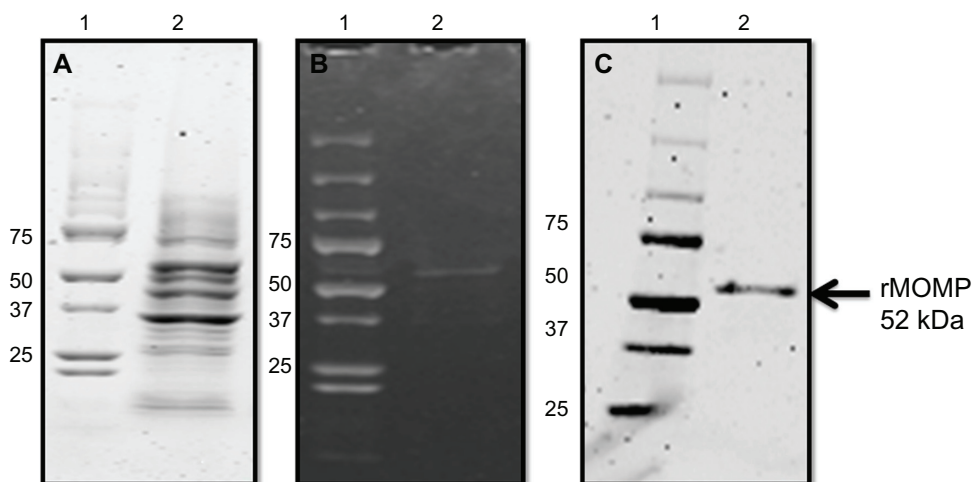


**Figure 1** Sodium dodecyl sulfate polyacrylamide gel electrophoresis and Western blot analyses of rMOMP. Sodium dodecyl sulfate polyacrylamide gel electrophoresis profiles of rMOMP (A) before (lane 2), and (B) after purification (lane 2) run on precast 4%–20% gradient gels, molecular weight marker (lane 1). (C) Western blot analysis of rMOMP, in which proteins were blotted onto a nitrocellulose membrane and probed with goat anti-MOMP antibodies (1:1000) followed by an Alexa Fluor 680 donkey anti-goat antibody (1:2000).

**Notes:** Bound antibody was visualized using an Odyssey imaging system. Molecular weight marker (lane 1) and purified rMOMP corresponding to approximately 52 kDa (lane 2).  
**Abbreviation:** rMOMP, recombinant major outer membrane protein.

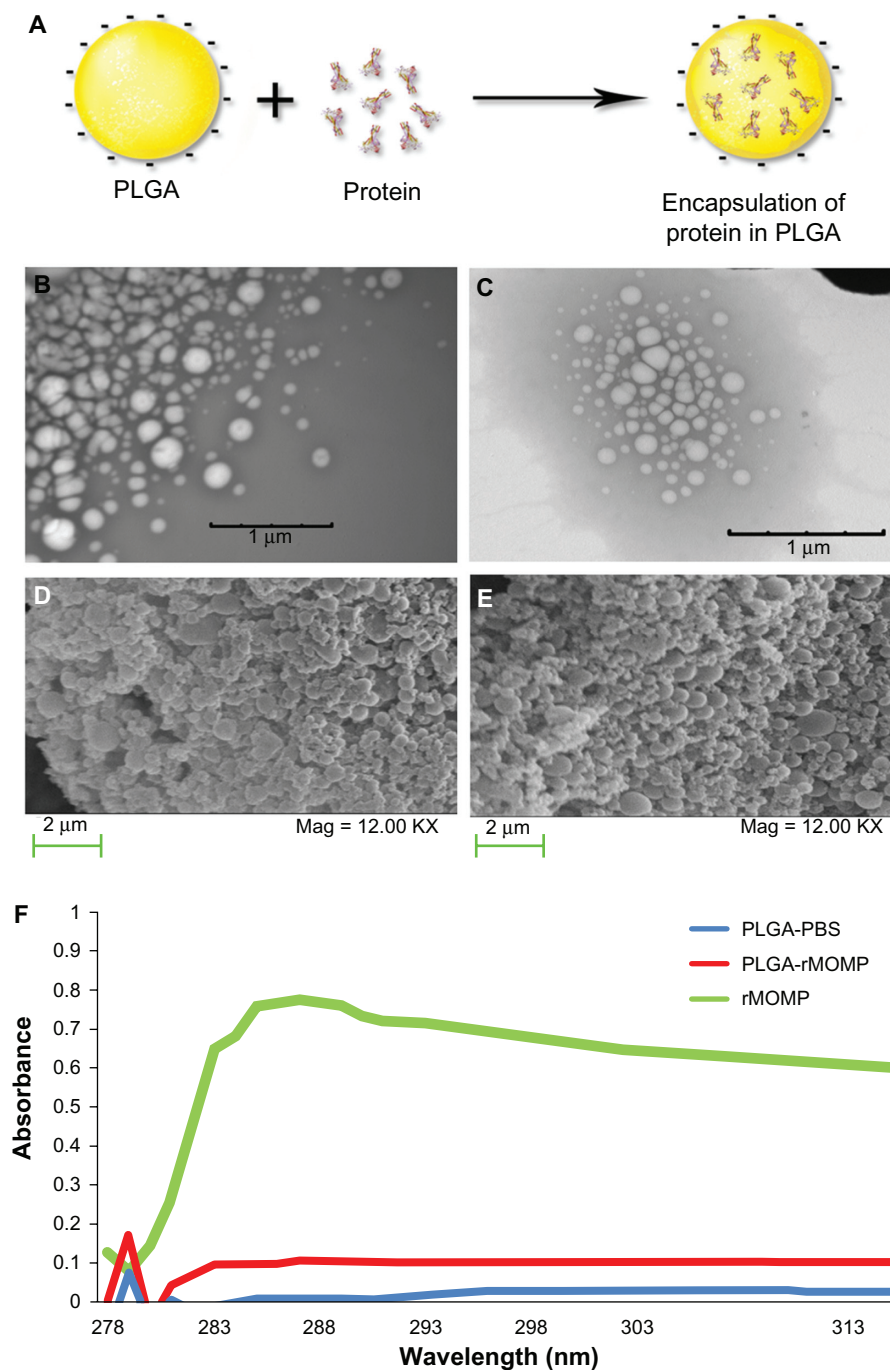


**Figure 2** Physical-structural characterization of PLGA nanoparticles. Schematic representation of rMOMP encapsulated in PLGA (**A**). The morphology and size of nanoparticles were observed using high-resolution TEM or SEM, where one drop of the nanoparticles was deposited on a copper grid or metal stub, respectively. The grids were allowed to dry for 10 minutes prior to imaging. The nanoparticles have a diameter of 100–300 nm for PLGA-PBS (**B** and **D**) and 300–500 nm for PLGA-rMOMP (**C** and **E**). Original magnification for SEM was 20 $\times$  and for TEM was 12 $\times$ . (**F**) Ultraviolet visualization absorbance spectra of rMOMP, PLGA-rMOMP, and PLGA-PBS were performed in deionized water at 25 $^{\circ}\text{C}$ .

**Abbreviations:** rMOMP, recombinant major outer membrane protein; PLGA, poly D, L-lactide-co-glycolide; PBS, phosphate-buffered saline; TEM, transmission electron microscopy; SEM, scanning electron microscopy.

the appearance of nanoparticles to be apparently more spherical with nanorange sizes (100–300 nm), corroborating the zetasizer results. The nanoparticles appeared to be smooth in shape and to have moderate uniformity. Further, as shown in Figure 2F, ultraviolet visualization of rMOMP

showed protein absorption at a wavelength of about 285 nm. In contrast, minimal to negligible absorption, respectively, was seen on the outer surface for PLGA-rMOMP and PLGA-PBS, further validating the successful encapsulation of rMOMP.

**Table 1** Nanoparticle size distribution, zeta potential, and encapsulation efficiency

Nanoparticles	Zeta size (nm)	Zeta potential (mV)	Encapsulation efficiency
PLGA-PBS	224 ± 46.7	-24.8 ± 2.5	?
PLGA-rMOMP	272 ± 48.85	-14.3 ± 0.8	60%

**Note:** Values are shown as the mean ± standard deviation for the zeta size and zeta potential.

**Abbreviations:** PLGA, poly D, L-lactide-co-glycolide; rMOMP, recombinant major outer membrane protein; PBS, phosphate-buffered saline.

## Release profile of rMOMP from PLGA nanoparticles

The cumulative release profile of rMOMP from PLGA-rMOMP nanoparticles over 15 days was one of a slight initial burst followed by sustained release (Figure 3A) that is characteristic for polymer systems, as recently shown for a rMOMP peptide.<sup>44</sup> Only 60% of the rMOMP was released over the entire time period, thus indicating its slow release pattern. Supernatants collected from the release studies were pooled and used for Western blotting to confirm the

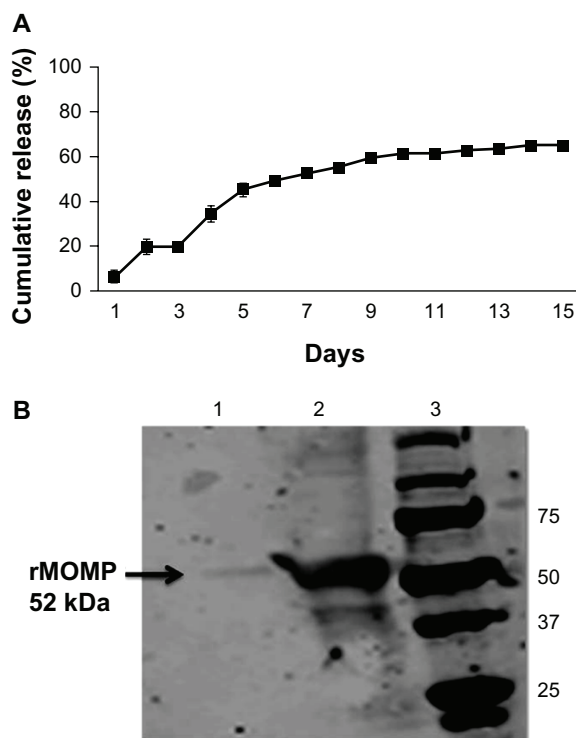


**Figure 3** In vitro release of rMOMP from encapsulated PLGA nanoparticles. **(A)** In vitro release of rMOMP from PLGA-rMOMP in phosphate-buffered saline containing 0.01% sodium azide incubated at 37°C. **(B)** Supernatants collected from the release studies were pooled and used for Western blotting by probing with anti-MOMP polyclonal antibodies; released rMOMP (lane 1); purified rMOMP (lane 2); molecular weight marker (lane 3).

**Note:** Arrow corresponds to rMOMP of approximately 52 kDa.

**Abbreviations:** rMOMP, recombinant major outer membrane protein; PLGA, poly D, L-lactide-co-glycolide.

specificity of the protein released. By probing with anti-MOMP polyclonal antibodies, it is evident (Figure 3B, lane 1) that a band at about 52 kDa was that of rMOMP. These studies serve as further confirmation of the successful encapsulation and release of rMOMP from PLGA nanoparticles.

## PLGA-rMOMP induces cytokines and chemokines in vitro

We first documented that PLGA-rMOMP could interact with macrophages by stimulating production of the IL-6 cytokine. Our results show that PLGA-rMOMP induced production of IL-6 by macrophages, which was not attributed to contamination by endotoxins because no differences were seen in IL-6 levels in the presence or absence of polymyxin B (Figure 4A). In contrast, IL-6 induced by lipopolysaccharide stimulation of macrophages was significantly ( $P < 0.05$ ) reduced in the presence of polymyxin B (Figure 4A). By employing confocal microscopy we further confirmed the slow release of encapsulated rMOMP by its ability to trigger the secretion of IL-6 (Figure 4B, red fluorescence) and IL-12p40 (Figure 4C, green fluorescence) in macrophages. No expression of IL-6 or IL-12p40 was observed in macrophages exposed to the PLGA-PBS control nanoparticles (data not shown).

Recently we reported that PLGA potentiated the ability of a rMOMP peptide to induce production of IL-6 and IL-12p40 cytokines by macrophages in vitro.<sup>44</sup> In this study, we documented that IL-12p40 was optimally induced in macrophages at a PLGA-rMOMP concentration of 100 ng/mL, but detected with a concentration as low as 10 ng/mL (Figure 4D). In comparison, a concentration of at least 1 µg/mL of purified rMOMP was needed to induce a similar level of IL-12p40 (Figure 4E). Neither PLGA-PBS nor unstimulated macrophages induced IL-12p40 (data not shown). These studies show the potentiating effect of PLGA on the capacity of the encapsulated rMOMP, at very low concentrations, to trigger production of IL-12p40 by mouse J774 macrophages.

To probe further the potential of PLGA-rMOMP as a candidate vaccine, we then evaluated its capacity to stimulate macrophages to produce other cytokines and chemokines, which are essential components of any protective immune response. We showed that mouse J774 macrophages stimulated with 100 ng/mL of PLGA-rMOMP produced significant ( $P \leq 0.05$ ) amounts of anti-inflammatory (IL-10) and proinflammatory (IL-1 $\alpha$  and tumor necrosis factor) cytokines (Figure 5A and B). In addition, the encapsulated rMOMP elicited significant ( $P \leq 0.05$ ) secretion of growth factor cytokines (granulocyte-macrophage colony-stimulating factor, IL-15, and granulocyte colony-stimulating factor,

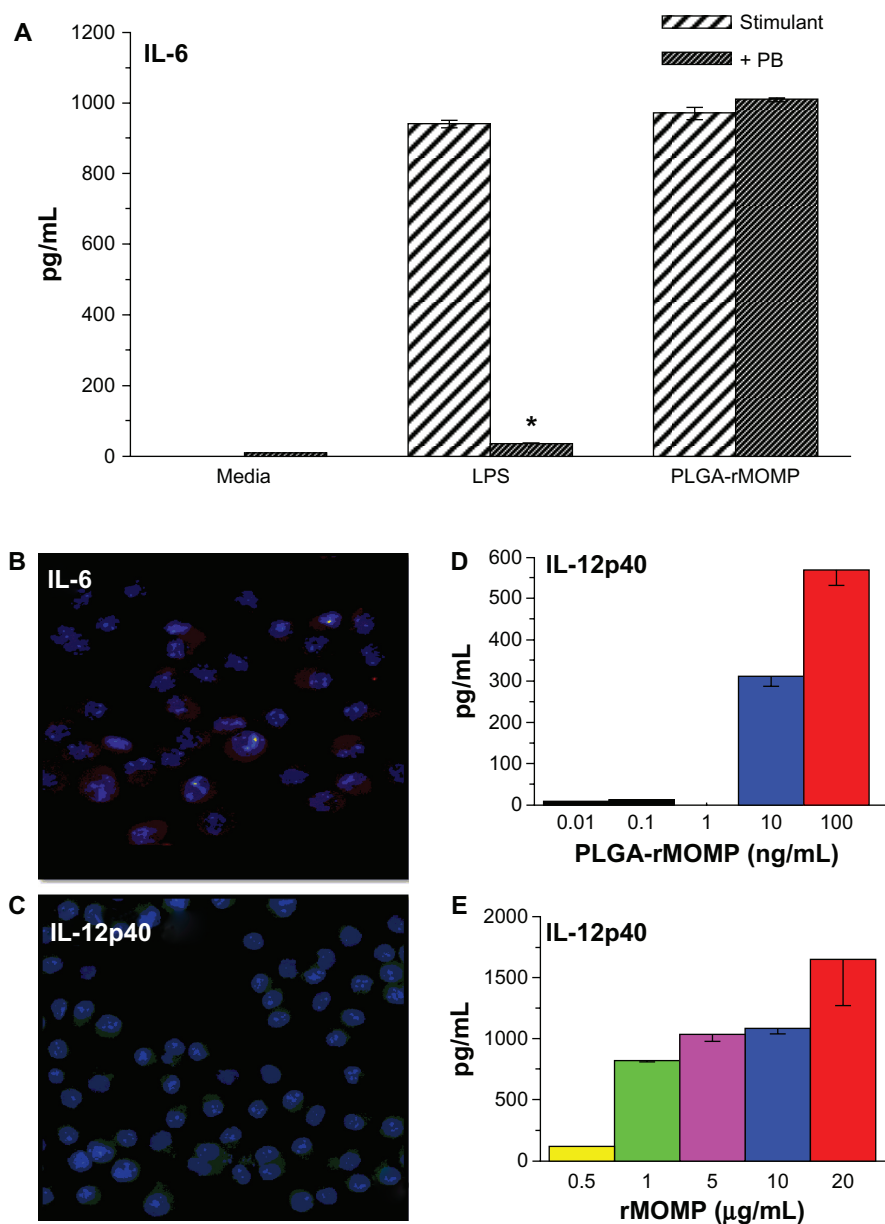


**Figure 4** PLGA-rMOMP stimulates production of cytokines by mouse J774 macrophages. **(A)** Macrophages ( $1 \times 10^6$ /mL) were seeded in 12-well plates and stimulated with PLGA-rMOMP (10  $\mu$ g/mL) in the presence and absence of polymyxin B at 10  $\mu$ g/mL for 24 hours at 37°C in a 5% CO<sub>2</sub> atmosphere. Stimulation of macrophages with lipopolysaccharide (1  $\mu$ g/mL) served as a control for these experiments. Cell-free supernatants were collected by centrifugation and used to quantify interleukin-6 using an antibody-capture specific enzyme-linked immunosorbent assay. Asterisk indicates significant differences ( $P < 0.05$ ) between levels of cytokine production in the presence and absence of polymyxin B. Each bar represents the mean  $\pm$  standard deviation of duplicate samples. **(B and C)** After 24 hours of stimulating macrophages ( $1 \times 10^5$ /well) in eight-well chamber slides with PLGA-rMOMP or PLGA-PBS, macrophages were fixed, and stained with either a PE antimouse interleukin-6 (shown in red) or FITC-antimouse IL-12 (shown in green) antibody, and nuclei were counterstained with 4',6-diamidino-2-phenylindole (DAPI, shown in blue). **(D and E)** Macrophages were visualized using confocal fluorescence microscopy at a magnification of 20 $\times$ . Macrophages ( $1 \times 10^5$ /mL) were stimulated with various concentrations of PLGA-rMOMP (0.01, 0.10, 1, 10, and 100 ng/mL), PLGA-PBS (data not shown), or purified rMOMP (0.5, 1, 5, 10, and 20  $\mu$ g/mL). After 24 hours, cell-free supernatants were harvested from culture medium and analyzed for interleukin-12p40 by antibody-capture specific enzyme-linked immunosorbent assays. Each bar represents the mean  $\pm$  standard deviation of duplicate samples representative of two independent experiments.

**Abbreviations:** PLGA, poly D, L-lactide-co-glycolide; rMOMP, recombinant major outer membrane protein; LPS, lipopolysaccharide; PB, polymyxin B; IL, interleukin; IL-12p40, interleukin (IL) 12 subunit beta 40.

Figure 5A and B) and copious levels of chemokines (CCL4, CCL2, CXCL10, CXCL5, and CCL5, Figure 5C and D). The PLGA-PBS control nanoparticles induced very weak and nonsignificant levels of IL-1 $\alpha$ , tumor necrosis factor, CCL2, and CCL4 (Figure 5A, B, and D). Spontaneous production of

IL-15 (Figure 5A) and CXCL10 (Figure 5C) by macrophages was also observed. Overall, the above experiments demonstrate the immunostimulatory potential of PLGA-rMOMP via its ability to trigger production of several major cytokines and chemokines by macrophages in vitro.

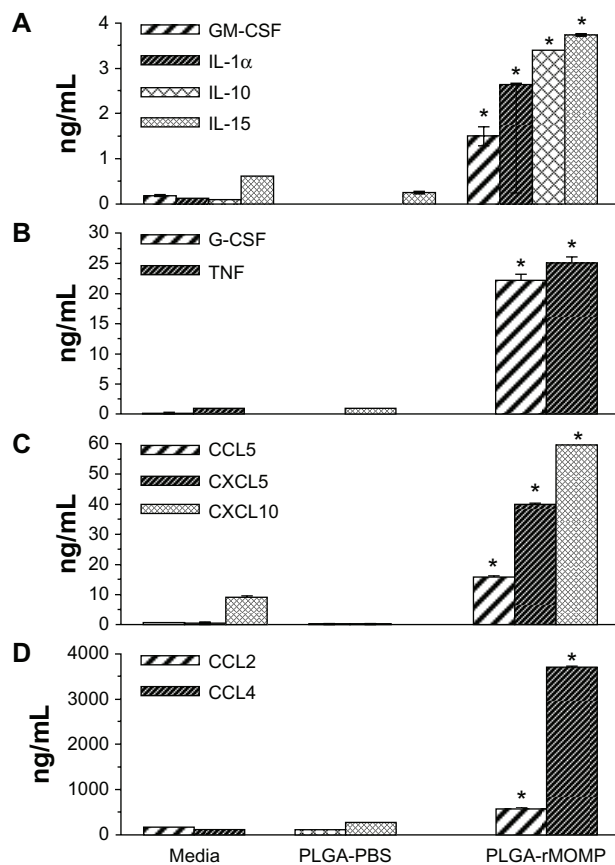


**Figure 5** PLGA-rMOMP stimulates production of cytokines and chemokines by mouse J774 macrophages.

**Notes:** Macrophages were stimulated with PLGA-rMOMP (100 ng/mL) and incubated as in Figure 4. Cell-free supernatants were collected by centrifugation and used to quantify cytokines (A and B) and chemokines (C and D) using a multiplex enzyme-linked immunosorbent assay. Asterisk indicates a significant difference in comparison with corresponding control ( $P < 0.05$ ). Each bar represents the mean  $\pm$  standard deviation of duplicate samples representative of two independent experiments.

**Abbreviations:** PLGA, poly D, L-lactide-co-glycolide; PBS, phosphate-buffered saline; rMOMP, recombinant major outer membrane protein; GM-CSF, granulocyte-macrophage colony-stimulating factor; IL, interleukin; G-CSF, granulocyte colony-stimulating factor; TNF, tumor necrosis factor; CCL5, chemokine (C-C motif) ligand 5; CXCL5, chemokine (C X C motif) ligand 5; CXCL10, chemokine (C X C motif) ligand 10; CCL2, chemokine (C-C motif) ligand 2; CCL4, chemokine (C-C motif) ligand 4.

## PLGA-rMOMP triggers elevated numbers of T cell subsets and Th1 cytokines in vivo

To evaluate the immunogenicity of the encapsulated rMOMP in vivo, groups of mice were immunized subcutaneously with PLGA-rMOMP, PLGA-PBS, or phosphate-buffered saline, and spleen cells were then collected for analysis of cellular responses. Our flow cytometry results revealed that ex vivo spleen cells from PLGA-rMOMP-immunized mice contained elevated numbers of CD4+ and CD8+ (34.82% and 14.77%, respectively) T cell subsets when compared with mice given PLGA-PBS (22.19% and 8.99%) or those given phosphate-buffered saline (24.91% and 9.83%, Figure 6). These findings indicate that

encapsulated rMOMP stimulates the expansion of CD4+ and CD8+ T cells in vivo.

Given that Th1 cytokines are considered mandatory prerequisites for a desirable *C. trachomatis* vaccine, we next evaluated the capacity of PLGA-rMOMP to trigger production of select key Th1 cytokines in mice. Spleen cells from groups of immunized mice were restimulated with purified rMOMP, and cell-free supernatants were used to quantify IL-12p40 (Th1/Th17) and IFN- $\gamma$  (Th1), as well as IL-4 (Th2) and IL-10 (Th2) cytokines using specific enzyme-linked immunosorbent assays. Spleen cells from PLGA-rMOMP-immunized mice produced significantly ( $P \leq 0.05$ ) more IL-12p40 (Figure 7A) and more IFN- $\gamma$  (Figure 7B) when restimulated with purified rMOMP at both 5  $\mu$ g and 10  $\mu$ g per mL as compared with the control groups of mice. Stimulated spleen cells from PLGA-rMOMP-immunized mice also secreted significant ( $P < 0.05$ ) amounts of IL-10 (Figure 7C), but at lower levels in comparison with IL-12p40 and in particular IFN- $\gamma$ . IL-4 was undetectable (detection level 7.8 pg/mL) in the supernatants from all groups of mice (data not shown). These results confirm the induction of a predominantly Th1 cytokine response triggered by encapsulated rMOMP in mice.

## PLGA-rMOMP triggers elevated Th1 antibody responses in vivo

Because antibodies are also of fundamental significance for protective immunity against *C. trachomatis*, we collected pooled sera from all the groups of mice after the final immunization to measure the isotypes and titers of rMOMP-specific antibodies by enzyme-linked immunosorbent assay. Mice immunized with PLGA-rMOMP produced IgG, IgG2a (Th1), and IgG1 (Th2) rMOMP-specific antibodies, which were present in significantly ( $P \leq 0.05$ ) greater amounts than those produced by the PLGA-PBS control mice (Figure 8A). Moreover, levels of IgG2a were significantly ( $P \leq 0.05$ ) higher than those of IgG1, with an IgG1 to IgG2a ratio of 0.25, which is indicative of a primary Th1-driven antibody response. The levels of antibodies measured in sera from the phosphate-buffered saline group (data not shown) mirrored those in the PLGA-PBS group.

To define further the robustness of the rMOMP-specific antibodies, we next performed serial two-fold dilutions of sera to determine isotype-specific antibody titers. As shown in Figure 8B, sera from the PLGA-rMOMP mice had higher antibody titers overall to all isotypes in comparison with the control mice. Strikingly, PLGA-rMOMP elicited a 64-fold higher IgG2a than IgG1 antibody titer in immunized mice.

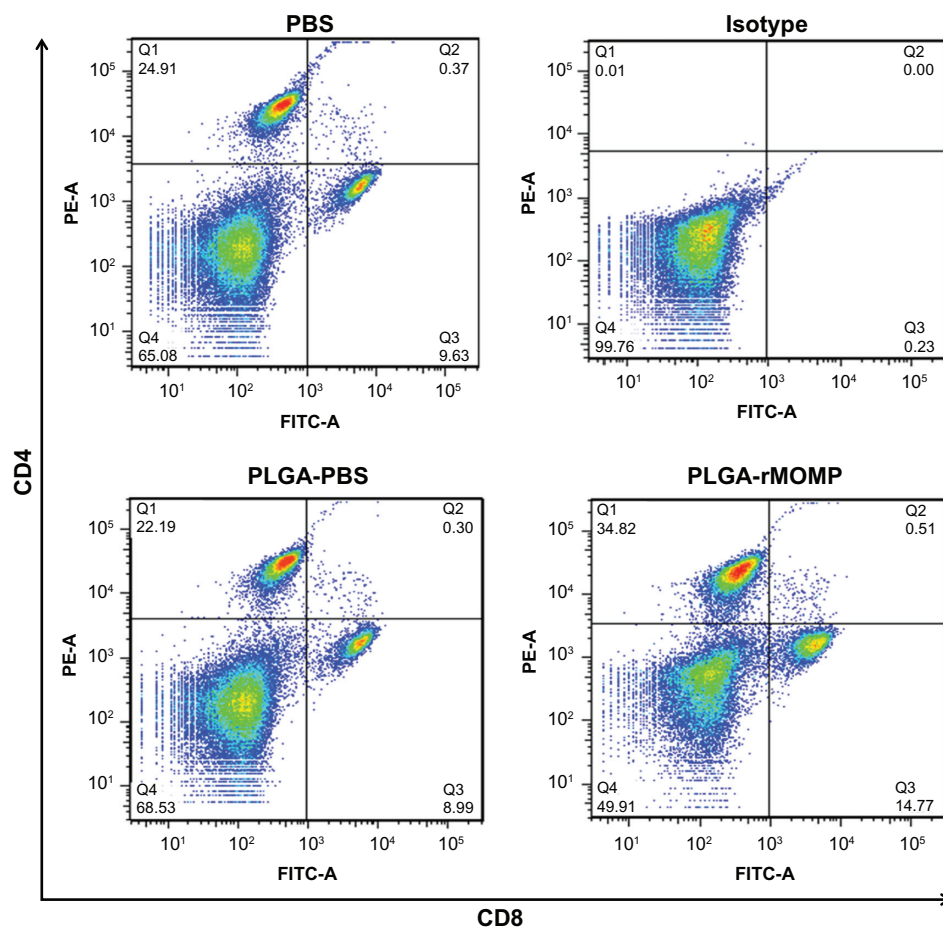


**Figure 6** Flow cytometric analyses of spleen CD4+ and CD8+ T cell subsets.

**Notes:** Groups of PLGA-rMOMP, PLGA-PBS, and PBS mice were immunized as indicated in the Materials and methods section. Spleen cells ( $1 \times 10^6/\text{mL}$ ) collected two weeks following the last immunization were used ex vivo to determine the percentages of CD4+ and CD8+ T cell subsets by flow cytometry. Shown are the percentages for CD4+ (Q1), CD4+CD8+ (Q2), CD8+ (Q3), and CD4-CD8- (Q4) cells for the various groups. The cells were stained with PE anti-CD4 and FITC anti-CD8 monoclonal antibody cocktail or with an isotype control cocktail antibody. Data were acquired on a BD FACS Canto II flow cytometer with at least  $1 \times 10^5$  events for each sample and analyzed using Flo Jo software.

**Abbreviations:** PLGA, poly D, L-lactide-co-glycolide acid; PBS, phosphate-buffered saline; rMOMP, recombinant major outer membrane protein; CD4, cluster of differentiation 4; CD8, cluster of differentiation 8.

To confirm the ability of the PLGA-rMOMP formulation to drive Th1 antibody responses, we also collected sera from mice following the same immunization regimen, but instead administered rMOMP in Freund's adjuvant to the mice. Our results show that sera from these mice produced heightened levels of IgG, IgG2a, and IgG1 rMOMP-specific antibodies (Figure 8C), but with an IgG1 to IgG2a ratio of 0.54. Results from the antibody titer study revealed only a four-fold higher IgG2a versus IgG1 antibody titer (Figure 8D). These findings confirm the ability of PLGA-rMOMP to drive not only Th1 cellular responses but also Th1 antibody responses, which are both potentiated by PLGA.

## Discussion

Development of a vaccine against *C. trachomatis* is considered to be the best way to prevent and control this

major bacterial sexually transmitted infection. Earlier first-generation vaccines focused on live, inactivated, or attenuated whole *C. trachomatis*,<sup>14–20</sup> which gave undesirable results and were associated with major pathological issues. Second-generation vaccines are subunit immunogens, such as proteins, DNA, RNA, or oligonucleotides, and have been shown to be very promising.<sup>21–35</sup> However, these second-generation vaccines need effective delivery systems to protect their respective immunogens from rapid degradation and to potentiate immunological responses. Biodegradable nanoparticles used as immune potentiators and delivery systems are now playing an increasing role in next-generation vaccine development projects.<sup>36–45</sup>

Previously we showed that a PLGA-encapsulated rMOMP peptide induced Th1 responses in vitro which were potentiated by the presence of PLGA,<sup>44</sup> suggesting that this

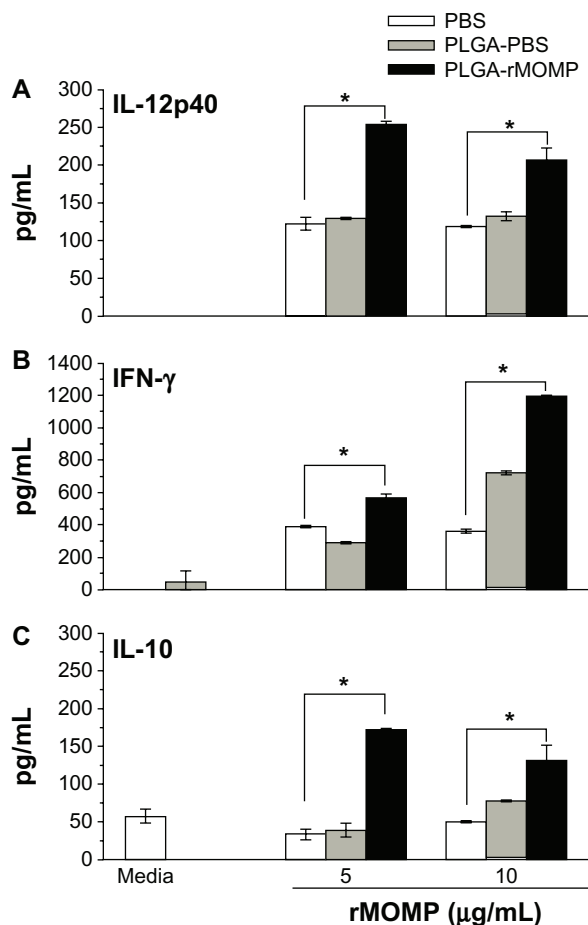


**Figure 7** Th1 and Th2 cytokine production by spleen cells from immunized mice. **Notes:** Mice in the PLGA-rMOMP and PLGA-PBS groups were immunized as indicated in the Materials and methods section. Spleen cells ( $3 \times 10^6$ /mL) collected from the mice two weeks following the last immunization were seeded in 24-well plates and stimulated with media or purified rMOMP (5 and 10  $\mu$ g/mL) for 24 hours at 37°C in a 5% CO<sub>2</sub> atmosphere. Cell-free supernatants were collected by centrifugation and used to quantify **A** and **B** Th1 (IL-12p40 and IFN- $\gamma$ ) and **C** Th2 (IL-10) cytokines using an antibody-capture specific enzyme-linked immunosorbent assay. Asterisk indicates a significant difference in comparison with the corresponding control ( $P < 0.05$ ). Each bar represents the mean  $\pm$  standard deviation of duplicate samples representative of two independent experiments.

**Abbreviations:** PLGA, poly D, L-lactide-co-glycolide acid; PBS, phosphate buffered saline; rMOMP, recombinant major outer membrane protein; IL, interleukin; IL-12p40, interleukin (IL) 12 subunit beta 40; IFN $\gamma$ , interferon gamma.

may be an effective delivery system for a *C. trachomatis* vaccine. In the present study, we explored further the effectiveness of PLGA as an immune potentiator and vaccine delivery system by encapsulating the full-length rMOMP in PLGA and investigating this formulation by in vitro and in vivo studies. Our results revealed the following: PLGA-rMOMP was smooth and spherical in shape, small in size at about 200–300 nm, with a zeta potential of  $-14.30$  mV, an encapsulation efficiency of about 60%, and a slow-release pattern; PLGA potentiated the ability of encapsulated rMOMP to trigger production of a variety of cytokines and chemokines by macrophages in vitro; PLGA-rMOMP

triggered expansion of T cell subsets and production of primarily rMOMP-specific Th1 cytokines in immunized mice; and sera from PLGA-rMOMP-immunized mice had increased levels of rMOMP-specific Th1 antibodies.

One concern with encapsulating proteins in PLGA using the w/o/w emulsion is the generation of heat, which poses a major risk to proteins, and increases the chances of instability, degradation, and interaction with organic solvents.<sup>43,50</sup> In the present study, addition of a stabilizer to the polymer suspension resulted in a high encapsulation efficiency and enabled a slow-release profile for the encapsulated rMOMP. A study by Jaganatha et al<sup>51</sup> showed that addition of stabilizers allows for a more stable encapsulant, higher encapsulation efficiency, and an extended and slow-release profile. Another concern regarding nanoparticle formulations is the value of the zeta potential, which is important for understanding and predicting the long-term stability and mucoadhesion of nanoparticles.<sup>52</sup> In theory, the more negative or positive the zeta potential, the more stable the nanoparticle suspension. Mucoadhesion, on the other hand, is promoted by the presence of positive charge groups.<sup>52</sup> Our results show that PLGA-rMOMP was stable and had a negative surface charge of  $-14.30$  mV, which may be attributed to the addition of polyvinyl alcohol to the suspension. A study by Kumar et al<sup>53</sup> showed that particles made with polyvinyl alcohol alone were negatively charged and those made with a blend of polyvinyl alcohol-chitosan were more positively charged.

The results of the release study also showed an initial burst release of rMOMP from PLGA-rMOMP followed by a gradual slow release, which is consistent with our previous study.<sup>44</sup> Most studies attribute an initial burst release to outer protein adsorption,<sup>54</sup> but our ultraviolet visualization data support that rMOMP is indeed encapsulated in the PLGA nanoparticle, and suggest that the initial burst and sustained release of rMOMP from PLGA-rMOMP may be due to the overall degradation kinetics of PLGA in solution.

Here, as documented, the release of rMOMP from PLGA was validated by its interaction with macrophages in triggering production of IL-6 and IL-12p40 cytokines, which are important in the host defense against chlamydial infection as well as other infections.<sup>7,55–58</sup> Further, PLGA potentiated production of selected IL-12p40 cytokines because a higher concentration of rMOMP was required to induce similar levels of this cytokine. Moreover, contamination by lipopolysaccharide was not responsible for production of these cytokines, as demonstrated in the polymyxin B experiments. It is of interest to note that our multiplex data also revealed significant secretion of several cytokines and chemokines. Although inflammation

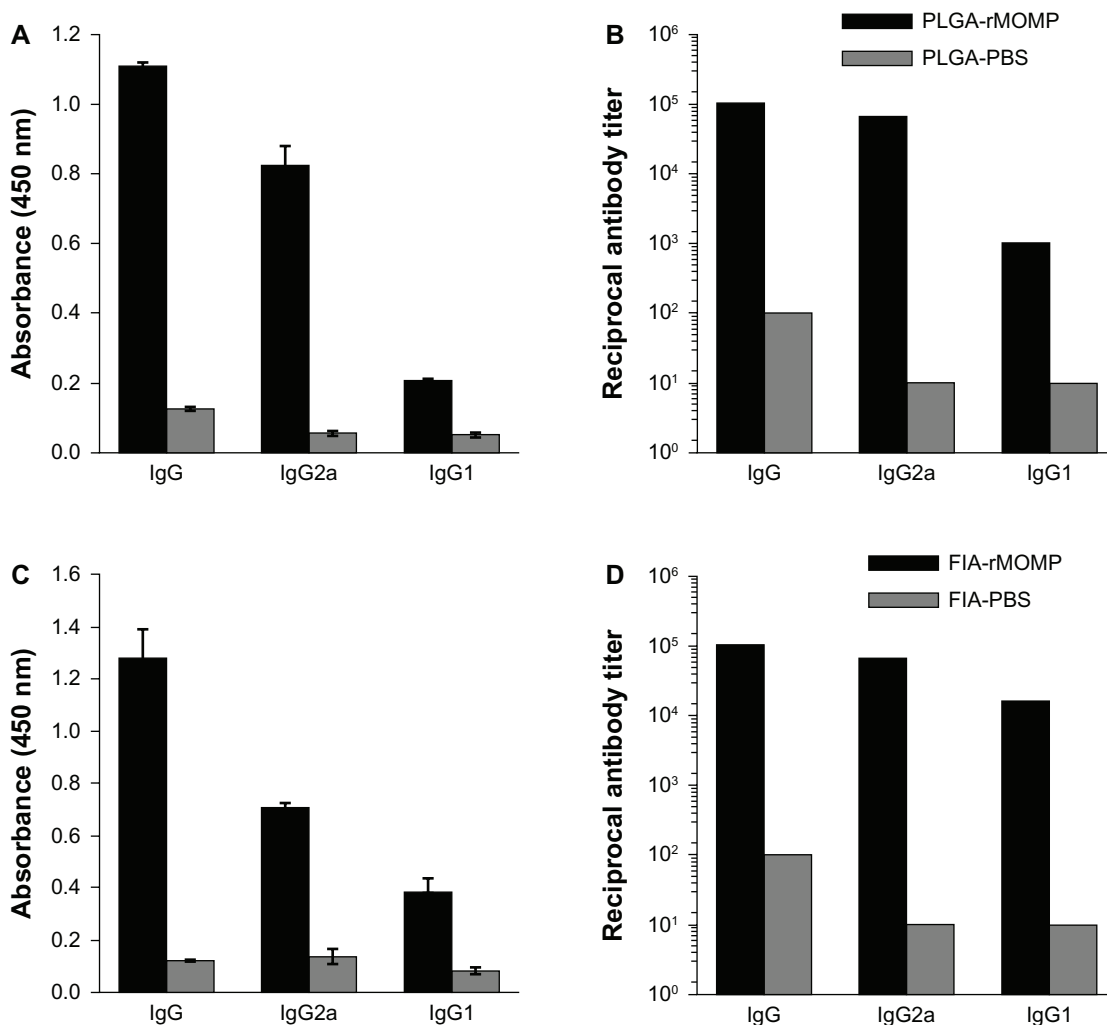


**Figure 8** Production of Th1 and Th2 antibodies in sera from immunized mice. (**A** and **B**) Groups of PLGA-rMOMP and PLGA-PBS mice were immunized as indicated in the Materials and methods section. Pooled sera were collected two weeks following the last immunization and used to determine IgG, IgG2a, and IgG1 responses in PLGA-rMOMP and PLGA-PBS mice at dilutions of 1:1600 and 1:100, respectively (**A**). Also shown are the reciprocal antibody titers for IgG, IgG2a, and IgG1 in PLGA-rMOMP and PLGA-PBS-immunized mice (**B**). (**C** and **D**) The groups of mice were immunized following the same immunization regimen as in the Materials and methods section, except rMOMP was administered to mice in FIA. Serum IgG, IgG2a and IgG1 responses (**C**) and reciprocal antibody titers (**D**) in FIA-PBS and FIA-rMOMP-immunized mice.

**Notes:** To determine antibody concentrations (titers), two-fold serial dilutions of serum were made and the endpoint titer was considered to be the last serum dilution with readings higher than the mean + 3 standard deviations of negative controls. Anti-rMOMP-specific antibodies were determined by enzyme-linked immunosorbent assay. Asterisk indicates a significant difference in comparison with the corresponding control ( $P < 0.05$ ). Each bar represents the mean  $\pm$  standard deviation of duplicate samples.

**Abbreviations:** PLGA, poly D, L-lactide-co-glycolide; PBS, phosphate-buffered saline; rMOMP, recombinant major outer membrane protein; FIA, Freund's incomplete adjuvant; IgG, immunoglobulin G.

is generally considered a double-edged sword, contributing to both host defense and tissue damage, in this study these proinflammatory cytokines (IL-1 $\alpha$ , tumor necrosis factor) and chemokines (CCL4, CCL2, CXCL10, CXCL5, CL5) played an active role in recruiting a variety of immune cells (monocytes, macrophages, neutrophils, natural killer cells, dendritic cells, and memory T cells) to the site of infection or inflammation.<sup>59,60</sup> Further, we observed significant secretion of granulocyte-macrophage colony-stimulating factor, IL-15, and granulocyte colony-stimulating factor, which stimulate cell growth factors, such as survival, proliferation, or differentiation of precursors needed by immune cells.<sup>59,60</sup>

These results corroborate the immunostimulatory and immune-potentiating properties of PLGA,<sup>39-44</sup> and indicate that PLGA-rMOMP could effectively activate T and B cells and induce humoral-mediated and cell-mediated immune responses in mice.

Activation and expansion of T cells is important in generating both humoral-mediated and cell-mediated immune responses, which are critical for limiting replication and clearance of intracellular pathogens.<sup>7,54-57</sup> In this study, we showed that encapsulation of rMOMP in PLGA 50:50 was effective in producing Th1 immune responses by proliferation of CD4+ and CD8+ subsets of T cells. Th1 cells such as

CD4+ and CD8+ enhance the cell-mediated immune response via synthesis of Th1 cytokines (IL-12p40 and IFN- $\gamma$ ) which are essential for resolving primary infection and/or resisting infection<sup>60–63</sup> via activation of phagocytes that limit the extent of infection. Lu and Zhong<sup>64</sup> observed that mice deficient in IL-12p40 failed to induce strong protection against chlamydial infection. Another study found that IFN- $\gamma$  receptor-deficient mice were unable to develop protective immunity against *C. trachomatis*.<sup>65</sup> Similar effects were also observed in IFN- $\gamma$  knockout mice which showed more disseminated and longer lasting *C. trachomatis* infection when compared with wild-type mice,<sup>66</sup> thus showing the importance of these cytokines in clearance of chlamydial infection. The high levels of production of IL-12p40 and IFN- $\gamma$  observed in the present study substantiates further the immunogenic potential of PLGA-rMOMP as a candidate nanovaccine.

Further assessment of isotype antibodies revealed that PLGA-rMOMP induced markedly higher levels of Th1 (IgG2a) than of Th2 (IgG1) rMOMP-specific antibodies, which was not observed in mice immunized with rMOMP in Freund's complete adjuvant. Stimulation of IgG2a antibody has been shown to be associated with protection against *Chlamydia* infection,<sup>67</sup> although the precise contribution of antibodies to this protection is still not completely understood. Nonetheless, strong evidence from studies does suggest that antibodies could play a role in resistance to reinfection<sup>68</sup> or in blocking attachment of *C. trachomatis* to epithelial cells.<sup>69</sup> Overall, the presence of predominantly Th1 immune responses triggered by PLGA-rMOMP in mice provides compelling evidence to suggest that perhaps these responses may be sufficient to render protective resistance against *C. trachomatis* infection.

Despite decades of effort in development of a *C. trachomatis* vaccine, there is still no effective vaccine against this pathogen. To our knowledge, our study is the first to document encapsulation of full-length rMOMP in PLGA 50:50 nanoparticles, to conduct physical-structural characterization studies, and to evaluate its immunogenicity comprehensively by both in vitro and in vivo experiments. Here we have documented that full rMOMP can be successfully encapsulated in PLGA using a variety of nanotechnology techniques. We show that PLGA potentiates the immune response because it enhances the ability of encapsulated rMOMP to trigger production of cytokines and chemokines in macrophages. Importantly, PLGA-rMOMP was found to be immunogenic in mice because it stimulated expansion of T cells and heightened T cell and B cell Th1 immune responses, which are all desirable for protective immunity against *C. trachomatis*.

Our data highlight the effectiveness of PLGA as a delivery system for development of a *C. trachomatis* vaccine. PLGA-rMOMP holds promise as a candidate nanovaccine, and warrants efficacy studies in mice.

## Acknowledgments

This research was supported by grants from the National Science Foundation NSF-CREST (HRD-1241701) and NSF-HBCU-UP (HRD-1135863). Special thanks to Yvonne Williams and Lashaundra Lucas from the Center for Nano-Biotechnology Research for their excellent administrative assistance. We also thank Eva Dennis for the PLGA illustration, and Michael Miller, Auburn University, for sequencing and assistance with SEM and TEM imaging.

## Disclosure

The authors report no conflicts of interest in this work.

## References

1. World Health Organization. Global prevalence and incidence of selected curable sexually transmitted infections: overviews and estimates. Geneva, Switzerland: World Health Organization; 2001. Available from: [http://www.who.int/hiv/pub/sti/who\\_hiv\\_aids\\_2001.02.pdf](http://www.who.int/hiv/pub/sti/who_hiv_aids_2001.02.pdf). Accessed April 19, 2013.
2. World Health Organization. Global strategy for prevention and control of sexually transmitted infections: 2006–2015. Geneva, Switzerland: World Health Organization; 2007. Available from: [http://apps.who.int/iris/bitstream/10665/43853/1/9789241563475\\_eng.pdf](http://apps.who.int/iris/bitstream/10665/43853/1/9789241563475_eng.pdf). Accessed April 19, 2013.
3. Centers for Disease Control and Prevention. Sexually transmitted disease surveillance, 2008. Atlanta, GA: Centers for Disease Control and Prevention; 2009. Available from: <http://www.cdc.gov/std/stats08/surv2008-complete.pdf>. Accessed April 19, 2013.
4. Norman J. Epidemiology of female genital *Chlamydia trachomatis* infections. *Best Pract Res Clin Obstet Gynaecol*. 2002;16:775–787.
5. Gonzales GF, Munoz G, Sanchez R, et al. Update on the impact of *Chlamydia trachomatis* infection on male fertility. *Andrologia*. 2004;36:1–23.
6. Stamm WE. *Chlamydia trachomatis* infections: progress and problems. *J Infect Dis*. 1999;179 Suppl 2:S380–S383.
7. Stamm W. *Chlamydia trachomatis* infections of the adult. In: Holmes KK, Sparling PF, Stamm WE, et al, editors. *Sexually Transmitted Diseases*. New York, NY: McGraw Hill Book Co; 2008.
8. Miyairi I, Ramsey KH, Patton DL. Duration of untreated chlamydial genital infection and factors associated with clearance: review of animal studies. *J Infect Dis*. 2010;201 Suppl 2:S96–S103.
9. Ibrahim AA, Refeidi A, El Mekki AA. Etiology and clinical features of acute epididymo-orchitis. *Ann Saudi Med*. 1996;16:171–174.
10. Taylor-Robinson D, Thomas BJ. The role of *Chlamydia trachomatis* in genital-tract and associated diseases. *J Clin Pathol*. 1980;33:205–233.
11. Tavakoli M, Craig AM, Malek M. An econometric analysis of screening and treatment of patients with suspected chlamydia. *Health Care Manag Sci*. 2002;5:33–39.
12. Wallester S, Salkeld G, Donovan B. The cost effectiveness of screening for genital *Chlamydia trachomatis* infection in Australia. *Sex Health*. 2006;3:225–234.
13. Honey E, Augood C, Templeton A, et al. Cost effectiveness of screening for *Chlamydia trachomatis*: a review of published studies. *Sex Transm Infect*. 2002;78:406–412.

14. Stagg AJ. Vaccines against chlamydia: approaches and progress. *Mol Med Today*. 1998;4:166–173.
15. Shewen PE, Povey RC, Wilson MR. A comparison of the efficacy of a live and four inactivated vaccine preparations for the protection of cats against experimental challenge with *Chlamydia psittaci*. *Can J Comp Med*. 1980;44:244–251.
16. Longbottom D, Livingstone M. Vaccination against chlamydial infections of man and animals. *Vet J*. 2006;171:263–275.
17. Su H, Messer R, Whitmire W, Hughes S, Caldwell HD. Subclinical chlamydial infection of the female mouse genital tract generates a potent protective immune response: implications for development of live attenuated chlamydial vaccine strains. *Infect Immun*. 2000;68:192–196.
18. Yu H, Karunakaran KP, Kelly I, et al. Immunization with live and dead *Chlamydia muridarum* induces different levels of protective immunity in a murine genital tract model: correlation with MHC class II peptide presentation and multifunctional Th1 cells. *J Immunol*. 2011;186:3615–3621.
19. Schachter J, Dawson C. *Human Chlamydial Infections*. Littleton, MA: PSG Publishing Co; 1978.
20. Grayston JT, Wang S. New knowledge of chlamydiae and the diseases they cause. *J Infect Dis*. 1975;132:87–105.
21. Eko FO, He Q, Brown T, et al. A novel recombinant multisubunit vaccine against chlamydia. *J Immunol*. 2004;173:3375–3382.
22. Pal S, Peterson EM, de la Maza LM. Vaccination with the *Chlamydia trachomatis* major outer membrane protein can elicit an immune response as protective as that resulting from inoculation with live bacteria. *Infect Immun*. 2005;73:8153–8160.
23. Pal S, Theodor I, Peterson E, et al. Immunization with *Chlamydia trachomatis* mouse pneumonitis major outer membrane protein can elicit a protective immune response against a genital challenge. *Infect Immun*. 2001;69:6240–6247.
24. Rockey D, Wang J, Lei L, et al. Chlamydia vaccine candidates and tools for chlamydial antigen discovery. *Expert Rev Vaccines*. 2009;8:1365–1377.
25. de la Maza LM, Peterson EM. Vaccines for *Chlamydia trachomatis* infections. *Curr Opin Investig Drugs*. 2002;3:980–986.
26. Baehr W, Zhang YX, Joseph T, et al. Mapping antigenic domains expressed by *Chlamydia trachomatis* major outer membrane protein genes. *Proc Nat Acad Sci U S A*. 1988;85:4000–4004.
27. Ortiz L, Demick KP, Petersen JW, et al. *Chlamydia trachomatis* major outer membrane protein (MOMP) epitopes that activate HLA class II-restricted T cells from infected humans. *J Immunol*. 1996;157:4554–4567.
28. Cheng C, Bettahi I, Cruz-Fisher MI, et al. Induction of protective immunity by vaccination against *Chlamydia trachomatis* using the major outer membrane protein adjuvanted with CpG oligodeoxynucleotide coupled to the nontoxic B subunit of cholera toxin. *Vaccine*. 2009;27:6239–6246.
29. Cunningham KA, Carey AJ, Lycke N, et al. CTA1-DD is an effective adjuvant for targeting anti-chlamydial immunity to the murine genital mucosa. *J Reprod Immunol*. 2009;81:34–38.
30. Sun G, Pal S, Weiland J, et al. Protection against an intranasal challenge by vaccines formulated with native and recombinant preparations of the *Chlamydia trachomatis* major outer membrane protein. *Vaccine*. 2009;27:5020–5025.
31. Igietseme JU, Murdin A. Induction of protective immunity against *Chlamydia trachomatis* genital infection by a vaccine based on major outer membrane protein lipophilic immune response-stimulating complexes. *Infect Immun*. 2000;68:6798–6806.
32. Pal S, Peterson EM, Rappuoli R, et al. Immunization with the *Chlamydia trachomatis* major outer membrane protein, using adjuvants developed for human vaccines, can induce partial protection in a mouse model against a genital challenge. *Vaccine*. 2006;24:766–775.
33. Pal S, Luke CJ, Barbour AG, et al. Immunization with the *Chlamydia trachomatis* major outer membrane protein, using the outer surface protein A of *Borrelia burgdorferi* as an adjuvant, can induce protection against a chlamydial genital challenge. *Vaccine*. 2003;21:1455–1465.
34. Berry LJ, Hickey DK, Skelding KA, et al. Transcutaneous immunization with combined cholera toxin and CpG adjuvant protects against *Chlamydia muridarum* genital tract infection. *Infect Immun*. 2004;72:1019–1028.
35. Singh SR, Hulett K, Pillai SR, et al. Mucosal immunization with recombinant MOMP genetically linked with modified cholera toxin confers protection against *Chlamydia trachomatis* infection. *Vaccine*. 2006;24:1213–1224.
36. Morlock M, Kolls H, Winter G, et al. Microencapsulation of rh-erythropoietin, using biodegradable poly(D,L-lactide-co-glycolide): protein stability and the effects of stabilizing excipients. *Eur J Pharm Biopharm*. 1997;43:29–36.
37. Takada S, Yamagata Y, Misaki M, et al. Sustained release of human growth hormone from microcapsules prepared by a solvent evaporation technique. *J Control Release*. 2003;88:229–242.
38. Lam XM, Duenas ET, Daugherty AL, et al. Sustained release of recombinant human insulin-like growth factor-I for treatment of diabetes. *J Control Release*. 2000;67:281–292.
39. Rosas JE, Pedraz JL, Hernandez RM, et al. Remarkably high antibody levels and protection against *P. falciparum* malaria in Aotus monkeys after a single immunization of SPf66 encapsulated in PLGA microspheres. *Vaccine*. 2002;20:1707–1710.
40. Audran R, Men Y, Johansen P, et al. Enhanced immunogenicity of microencapsulated tetanus toxoid with stabilizing agents. *Pharm Res*. 1998;15:1111–1116.
41. Igartua M, Hernandez RM, Esquisabel A, et al. Enhanced immune response after subcutaneous and oral immunization with biodegradable PLGA. *J Control Release*. 1998;56:63–73.
42. Carcaboso AM, Hernandez RM, Igartua M, et al. Immune response after oral administration of the encapsulated malaria synthetic peptide SPf66. *Int J Pharm*. 2003;260:273–282.
43. Lima KM, Rodrigues JM. Poly-DL-lactide-co-glycolide microspheres as a controlled release antigen delivery system. *Braz J Med Biol Res*. 1999;32:171–180.
44. Taha M, Singh SR, Dennis VA. Biodegradable PLGA 85/15 nanoparticles as a delivery vehicle for *Chlamydia trachomatis* recombinant MOMP-187 peptide. *Nanotechnology*. 2012;23:325101.
45. Boyoglu S, Vig K, Pillai S, et al. Enhance delivery of nanoencapsulated DNA vaccine vector for respiratory syncytial virus. *Nanomedicine*. 2009;5:463–472.
46. Champion CI, Kickhoefer VA, Liu G, et al. A vault nanoparticle vaccine induces protective mucosal immunity. *PLoS One*. 2009;4:e5409.
47. Singh SR, Dennis VA, Carter CL, et al. Immunogenicity and efficacy of recombinant RSV-F vaccine in mouse model. *Vaccine*. 2007;25:6211–6223.
48. Singh SR, Dennis VA, Carter CL, et al. Respiratory syncytial virus recombinant F protein (residues 255–278) induces a helper T cell type 1 immune response in mice. *Viral Immunol*. 2007;20:261–275.
49. Taha M, Singh SR, Hulett K, et al. A peptide containing T-cell epitopes of *Chlamydia trachomatis* recombinant MOMP induces systemic and mucosal antibody responses in mice. *WJV*. 2011;1(4):138–147.
50. Raghavendra C, Mundargi V, Babu R, et al. Nano/micro technologies for delivering macromolecular therapeutics using poly (D, L-lactide-co-glycolide) and its derivatives. *J Control Release*. 2008;125:193–209.
51. Jaganatha KS, Rao YU, Singh P, et al. Development of a single dose tetanus toxoid formulation based on polymeric microspheres: a comparative study of poly(D, L-lactic-co-glycolic acid) versus chitosan microspheres. *Int J Pharm*. 2005;294:23–32.
52. Bayens V, Gurny R. Chemical and physical parameters of tears relevant for the design of ocular drug delivery formulations. *Pharm Acta Helv*. 1997;72:191–202.
53. Kumar MNV, Bakowsky U, Lehr CM. Preparation and characterization of cationic PLGA nanospheres as DNA carriers. *Biomaterials*. 2005;25:1771–1777.
54. Alonso MJ, Gupla RK, Mim C, et al. Biodegradable microspheres as controlled-release tetanus toxoid delivery systems. *Vaccine*. 1994;12:299–306.

55. Rasmussen SJ, Eckman L, Quayle AJ, et al. Secretion of proinflammatory cytokines by epithelial cells in response to chlamydia infection suggests a central role for epithelial cells in chlamydial pathogenesis. *J Clin Invest.* 1997;99:77–87.
56. Gupta R, Srivastava P, Vardhan H, et al. Host immune responses to chlamydial inclusion membrane proteins B and C in *Chlamydia trachomatis* infected women with and without fertility disorders. *Reprod Biol Endocrinol.* 2009;7:38.
57. Watford WT, Moriguchi M, Morinobu A, et al. The biology of IL-12: coordinating innate and adaptive immune responses. *Cytokine Growth Factor Rev.* 2003;14:361–368.
58. Williams DM, Grubbs BG, Darville T, et al. Role for interleukin-6 in host defense against murine *Chlamydia trachomatis* infection. *Infect Immun.* 1998;66:4464–4467.
59. Iwasaki A, Medzhitov R. Regulation of adaptive immunity by the innate immune system. *Science.* 2012;327:291–295.
60. Kaiko G, Horvat J, Beagley K, et al. Immunological decision making: how does the immune system decide to mount a helper T-cell response? *Immunology.* 2008;123:326–338.
61. Rottenberg ME, Rothfuchs ACG, Gigliotti D, et al. Role of innate and adaptive immunity in the outcome of primary infection with *Chlamydia pneumoniae*, as analyzed in genetically modified mice. *J Immunol.* 1999;162:2829–2836.
62. Rothfuch A, Kreuger M, Wigzell H, et al. Macrophages, CD4+ or CD8+ cells are each sufficient for protection against *Chlamydia pneumoniae* infection through their ability to secrete IFN-gamma. *J Immunol.* 2004;172:2407–2415.
63. Jupelli M, Guentzel M, Meier P, et al. Endogenous IFN-gamma production is induced and required for protective immunity against pulmonary chlamydial infection in neonatal mice. *J Immunol.* 2008;180:4148–4155.
64. Lu H, Zhong G. Interleukin production is required for chlamydial antigen-pulsed dendritic cells to induce protection against live *Chlamydia trachomatis* infection. *Infect Immun.* 1999;67:1763–1769.
65. Johansson M, Schon K, Ward M, et al. Genital tract infection *Chlamydia trachomatis* fails to induce protective immunity in gamma interferon receptor deficient mice despite a strong local immunoglobulin A response. *Infect Immun.* 1997;65:1032–1044.
66. Cotter TW, Ramsey KH, Miranpuri GS, et al. Dissemination of *Chlamydia trachomatis* chronic genital tract infection in gamma interferon gene knockout mice. *Infect Immun.* 1997;65:2145–2152.
67. Igietseme JU, Uriri IM, Kumar SN, et al. Route of infection that induces a high intensity of gamma interferon-secreting T cells in the genital tract produces optimal protection against *Chlamydia trachomatis* infection in mice. *Infect Immun.* 1998;66:4030–4035.
68. Igietseme JU, Eko FO, He Q, et al. Antibody regulation of T-cell immunity: implications for vaccine strategies against intracellular pathogens. *Expert Rev Vaccines.* 2004;3:23–34.
69. Pal S, Theodor I, Peterson EM, et al. Monoclonal immunoglobulin A antibody to the major outer membrane protein of the *Chlamydia trachomatis* mouse pneumonitis biovar protects mice against a chlamydial genital challenge. *Vaccine.* 1997;15:575–582.

## International Journal of Nanomedicine

### Publish your work in this journal

The International Journal of Nanomedicine is an international, peer-reviewed journal focusing on the application of nanotechnology in diagnostics, therapeutics, and drug delivery systems throughout the biomedical field. This journal is indexed on PubMed Central, MedLine, CAS, SciSearch®, Current Contents®/Clinical Medicine,

Submit your manuscript here: <http://www.dovepress.com/international-journal-of-nanomedicine-journal>

Dovepress

Journal Citation Reports/Science Edition, EMBase, Scopus and the Elsevier Bibliographic databases. The manuscript management system is completely online and includes a very quick and fair peer-review system, which is all easy to use. Visit <http://www.dovepress.com/testimonials.php> to read real quotes from published authors.